SIMULATION OF QUARK JET FRAGMENTATION INTO MESONS AND BARYONS ON THE BASIS OF A CHAIN DECAY MODEL

By S. Ritter and J. Ranft

Sektion Physik, Karl-Marx-Universität, Leipzig*

(Received September 18, 1979)

We present a Monte Carlo calculation for multiparticle events in e^+e^--annihilation. The underlying model is a chain decay model and has the following features: (*i*) Baryon production as well as meson production, (*ii*) Energy-momentum conservation, (*iii*) Conservation of quantum numbers like Q, I_3, S, B, (*iv*) Inclusion of transverse momentum of the emitted hadrons, (*v*) Fragmentation via meson and baryon resonances of the lowest SU(3) multiplets. We compare the results of the model with experimental data on e^+e^--annihilation including average multiplicities of charged and neutral particles, longitudinal and transverse momentum distributions of the final hadrons and distributions of jet variables like Thrust. In general the agreement of the model with experimental data is good.

1. Introduction

Presently, the multihadron production in high energy collisions is usually studied in the frame work of the quark parton model. We want to present a quark fragmentation model and apply this to e^+e^--annihilation into hadrons. This problem has been previously studied by Field and Feynman [1] and Ilgenfritz, Kripfganz and Schiller [2]. Despite of its phenomenological success the model of Field and Feynman suffers from several defects as already pointed out by the authors. These include: (*i*) The model does not conserve energy-momentum, (*ii*) The model does not predict baryon production, (*iii*) The model does not include the conservation of quantum numbers like Q, I_3, S, B.

The aim of our work was to develop a more realistic model which is able to overcome the above mentioned defects. In order to include (anti)baryon production we use the scheme of Ilgenfritz, Kripfganz and Schiller [2]. That means we consider beside (anti)quark jets also (anti)diquark jets.

The outline of the paper is the following: In Chapter 2 we give a short description of the quark fragmentation model, in Chapter 3 we describe the Monte Carlo model in detail and in Chapter 4 we compare the results of the model with experimental data.

* Address: Sektion Physik, Karl-Marx-Universität, Karl-Marx-Platz, 701 Leipzig, DDR.

2. The quark fragmentation model

Inclusive hadron production in e^+e^--annihilation and lepton hadron collisions is usually studied in the quark parton model in terms of the quark fragmentation functions $D_q^h(z)$. $D_q^h(z)$ is the probability distribution for finding a hadron of the type h in the jet resulting from the fragmentation of the quark q. $z = P_{\text{hadron}}/P_{\text{jet}}$ is the momentum fraction of the hadron. Scale violations of the quark fragmentation functions like those following from QCD are not considered in the present paper. It is not obvious how to include scale violations in chain decay models like the one considered here. At present there is no reliable method to calculate the quark fragmentation functions from an underlying theory, say QCD. Therefore phenomenological chain decay models have been developed [1–3]. In their simplest version the quark fragmentation functions $D(z)$ are given as a solution of the integral equation

$$D(z) = d(z) + \int_0^{1-z} \frac{dz'}{1-z'}\, d(z') D\left(\frac{z}{1-z'}\right) \tag{1}$$

first studied by Finkelstein and Peccei [4] and Krzywicki and Peterson [5]. $z = P_{\parallel \text{ hadron}}/P_{\text{jet}}$ is the scaling variable. In equation (1) transverse momenta and masses of the quarks and final hadrons are neglected. Therefore the momentum P_{jet} of the original quark jet is equal to its energy $\sqrt{s}/2$. $d(z)$ is the so called momentum sharing function or vertex function. $d(z)dz$ gives the probability to emit in the first step a hadron with the momentum fraction z in dz. The first emitted hadron leaves behind a remaining jet with the probability $d(1-\eta)d\eta$ where $\eta = 1-z$. Each hadron considered is either emitted in the first step or results from the fragmentation of the remaining jet. In the second case $D(z/\eta)$ is the distribution of the hadrons with the rescaled momentum fraction z/η within the remaining jet. The integral equation (1) is unrealistic for low initial energies $\sqrt{s}/2$ since it provides quark fragmentation functions $D(z)$ which scale at each initial energy.

Equation (1) is underlying the following simple model. A quark of the type a has a determined initial momentum p_0 in the z-direction. This quark creates a new quark antiquark pair of the type $b\bar{b}$. The original quark a recombines with the antiquark $\bar{b}$ to one meson of the type $a\bar{b}$ with the momentum fraction $z_{h_1} = p_{h_1}/p_0$ and leaves behind the quark b which carries the momentum fraction $\eta_1 = p_1/p_0 = (p_0 - p_{h1})/p_0 = 1 - z_{h1}$. The quark b creates a further quark antiquark pair of the type $c\bar{c}$ and so on.

Later we discuss a method to include transverse momenta in the model. In a Monte Carlo model of this kind the chain decay must stop as soon as the momentum of the incoming jet is too low. In case that the fragmentation of a single quark is considered the momentum cannot be conserved exactly since there always exists a residual jet with some small momentum. But if the initial momentum p_0 is sufficiently high then the residual jet carries only a small fraction of the initial momentum and we have approximate momentum conservation. Including diquark and antidiquark jets the model can easily be expanded to describe also baryon and antibaryon production beside the meson production. Using the integral equation method this has been discussed in the paper by Ilgenfritz, Kripfganz and Schiller [2].

In figures 1 and 2 we illustrate chain decays containing only mesons and mesons and (anti)baryons, respectively.

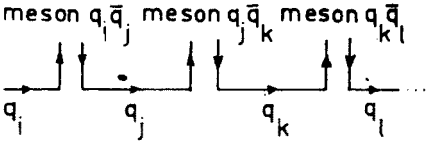

Fig. 1. Chain decay into only mesons. i, j, l are the flavour quantum numbers of the quarks q and antiquarks $\bar{q}$

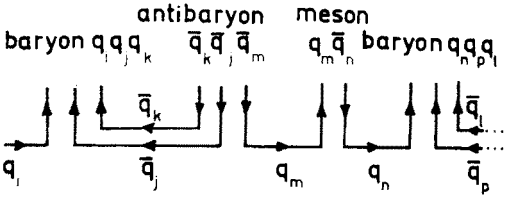

Fig. 2. Chain decay into mesons and baryons. i, j, k, l, m, n, p are the flavour quantum numbers of the quarks and antiquarks

We review briefly the solution of the chain decay equation by Ilgenfritz, Kripfganz and Schiller [2] and discuss the asymptotic behaviour. First we neglect for simplicity the quantum number structure of the jet and use the vertex function

$$d(z) = (\beta+1)\,(1-z)^{\beta} \tag{2}$$

with the normalization condition

$$\int_0^1 d(z)dz = 1. \tag{3}$$

The solution of the integral equation (1) is

$$D(z) = \frac{\beta+z}{z}\,(1-z)^{\beta}. \tag{4}$$

The distribution for non-leading particles, that are particles not emitted in the first step, is

$$D^{\mathrm{NL}}(z) = D(z)-d(z) = (\beta+1)\,(1-z)^{\beta+1}/z. \tag{5}$$

In more general cases the equation is solved by Mellin transformation. In order to include quantum numbers a transition matrix $R_{qq'}$ is defined.

$$R_{qq'} = \sum_{h} R^{h}_{qq'} \quad \text{with} \quad R^{h}_{qq'} = 0 \quad \text{for} \quad h \neq q\bar{q}'. \tag{6}$$

$R^{h}_{qq'}$ gives the probability that the incoming quark jet q emits a hadron of the type h and leaves behind a quark jet q'. The transition matrix is normalized according to

$$\sum_{q'} R_{qq'} = 1. \tag{7}$$

The sum goes over all considered quark flavours. Considering only the lowest SU(3) multiplets, the pseudoscalar and vector meson nonet, we have the transition matrix

$$\sum_{h} hR^{h}_{qq'} = \frac{\alpha}{(2+\kappa)}\begin{bmatrix} \frac{1}{2}(\pi^0+\eta\cos^2\theta+\eta'\sin^2\theta) & \pi^+ & \\ \pi^- & & \frac{1}{2}(\pi^0+\cos^2\theta\eta+\sin^2\theta\eta') \\ K^- & & \bar{K}^0 \\ \kappa K^+ & & \\ \kappa K^0 & & \\ (\eta\sin^2\theta+\eta'\cos^2\theta) & & \end{bmatrix} + \frac{\alpha_V}{(2+\kappa)}\begin{bmatrix} \frac{1}{2}(\varrho^0+\omega) & \varrho^+ & \kappa K^{*+} \\ \varrho^- & \frac{1}{2}(\varrho^0+\omega) & \kappa K^{*0} \\ K^{*-} & \bar{K}^{*0} & \kappa\phi \end{bmatrix}. \tag{8}$$

The ratios between the coupling constants $R^{h}_{qq'}$ of the same multiplet are given by the Clebsch–Gordan coefficients. The ratios between different multiplets are specified by weights α_{PS}, α_V with $\alpha_{PS}+\alpha_V = 1$. SU(6) symmetry suggests $\alpha_V/\alpha_{PS} = 3$. θ is the mixing angle between the singlet and octet members of the multiplet and $\kappa \leqslant 1$ suppresses strange particle production. If we write down only the coefficients of the transition matrix we get in the SU(3) case

$$R_{qq'} = \frac{1}{(2+\kappa)}\begin{bmatrix} 1 & 1 & \kappa \\ 1 & 1 & \kappa \\ 1 & 1 & \kappa \end{bmatrix}. \tag{9}$$

We see here no reason to follow the arguments used by Sukhatme [6, 7] who assumes a symmetrical transition matrix like

$$R_{qq'} = \frac{1}{5}\begin{bmatrix} 2 & 2 & 1 \\ 2 & 2 & 1 \\ 1 & 1 & 3 \end{bmatrix}. \tag{10}$$

Finally we discuss the asymptotic behaviour of the model for large initial momenta. We get a logarithmic multiplicity rise with the initial momentum p

$$\langle n_{q/h}\rangle = \int_{z_0=\mu/p}^{1} dz D^{h}_{q}(z) \sim 2\sum_{q'} R_{qq'}R^{h}_{q,q'\bar{h}}\left\{\log\frac{p}{\mu}\right\}, \tag{11}$$

p is the initial momentum of the jet and μ is in the order of the transverse mass $m_\perp$ of the emitted hadrons. From equation (11) we get the following asymptotical behaviour

$$\begin{aligned} \frac{\langle n_K\rangle}{\langle n_\pi\rangle} &= \frac{\langle n_{K^*}\rangle}{\langle n_\varrho\rangle} \xrightarrow[p\to\infty]{} \kappa, \\ \frac{\langle n_\varrho\rangle}{\langle n_\pi\rangle} &= \frac{\langle n_{K^*}\rangle}{\langle n_K\rangle} \xrightarrow[p\to\infty]{} \frac{\alpha_V}{\alpha_{PS}}, \end{aligned} \tag{12}$$

We extend furthermore the model to baryon and antibaryon production, include transverse momenta and quantum numbers like Q, I_3, S, B. The model is applied to multihadron production in hadronic $e^+e^- \to q_0\bar{q}_0$ annihilation processes. In this process each of the original quarks q_0 and $\bar{q}_0$ creates separately a hadron jet in the following manner: The original quark $q_0(\bar{q}_0)$ with the energy $\sqrt{s}/2$ and the momentum in $+(-)$ z-direction creates in the colour field between the $q\bar{q}$ pair one or two new quark antiquark pairs. If only one pair $q_1\bar{q}_1(q_1'\bar{q}_1')$ is created one meson $q_0\bar{q}_1(\bar{q}_0q_1')$ is emitted and a quark jet $\bar{q}_1$ (antiquark jet $\bar{q}_1'$) remains. If two pairs $q_1\bar{q}_1$ and $q_2\bar{q}_2$ are created one baryon $q_0q_1q_2$ (antibaryon $\bar{q}_0\bar{q}_1'\bar{q}_2'$) is emitted and an antiquark jet $\bar{q}_1\bar{q}_2$ (diquark jet $q_1'q_2'$) remains.

In figures 3 and 4 we represent these four vertices. The remaining jets create now one or two further quark antiquark pairs and so on. In this manner we generate first separately two hadron jets. At the end the two residual jets are combined. They may contain one or

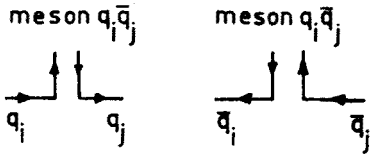

Fig. 3. Vertex for the emission of a meson from a quark jet and antiquark jet

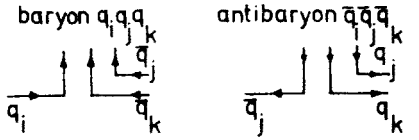

Fig. 4. Vertex for the emission of a baryon from a quark jet and an antibaryon from an antiquark jet

two mesons or one baryon or antibaryon. In figure 5 we show a possible vertex structure of a total jet after the combination of the two original jets. The flavours of the quarks in figure 5 were not specified. Each new $q\bar{q}$ pair gets a flavour quantum number. Details about

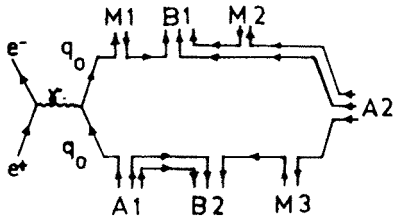

Fig. 5. Example for the vertex structure of one final hadronic state in e^+e^--annihilation. M, B and A stand for meson, baryon and antibaryon, respectively, $q_0\bar{q}_0$ is the primary quark antiquark pair and γ is the virtual photon

the flavour choice, energy and momentum selection are given in Section 3. In e^+e^--annihilation the possibilities for the flavours of the original quarks q_0 and $\bar{q}_0$ which couple on the virtual photon are determined by their squared charges. In the present version

of the model we consider only noncharmed hadrons. Neglecting contributions from heavy leptons we obtain for the probabilities that the original quarks carry the flavour $q\bar{q}$: $P_{d\bar{d}} = P_{s\bar{s}} = 1/6$ and $P_{u\bar{u}} = 2/3$.

3. Monte Carlo chain decay model

The simulation of a hadron jet in the process $e^+e^- \to \gamma \to q\bar{q} \to$ hadrons proceeds by the following steps. At the beginning we choose the e^+e^--collision energy and the initial quark flavour. The initial situation is symmetrical $E_q = E_{\bar{q}} = \sqrt{s}/2$ and $\vec{p}_q = -\vec{p}_{\bar{q}}$ and the original quarks carry no transverse momenta. In the following steps we generate first separately two hadron jets from the original quark q and antiquark $\bar{q}$.

(1) Check of the end of the chain situation: At the beginning of each emission step we compare the energy of the incoming quark jet with a randomly generated cut off energy. If the jet energy is less than the cut off energy we stop the further chain decay.

(2) Choice of the vertex: We sample randomly whether a meson or (anti)baryon should be emitted in the following emission step.

(3) Choice of the quark flavour: Here we have to sample the quark flavour of the newly created $q\bar{q}$ pair or of the newly created $q\bar{q}$ pairs, respectively.

(4) Hadron classification: In this step we classify the emitted hadron or hadron resonance according to the chosen vertex and quark flavours.

(5) Choice of the hadron energy: We sample the hadron energy and calculate the energy of the remaining jet.

(6) Choice of the transverse momentum: We choose the transverse momentum of the emitted hadron. The longitudinal momentum of this hadron is then determined by its mass, transverse momentum and energy.

$$p_{\parallel h} = \pm\sqrt{E_h^2 - m_h^2 - p_{\perp h}^2}\,, \tag{13}$$

where $+(-)$ is used for the hadrons created in the jet with the original quark q (antiquark $\bar{q}$).

(7) Combination of the two hadron jets: After having reached the end of chain situation for both jets we combine them to a hadron two-jet.

(8) Decay of the hadron resonances: In this step all resonances decay into the observed stable hadrons.

In the following sections we discuss the above steps in more detail.

3.1. Check of the end of chain situation

We choose randomly a cut off energy $E_{\text{cut off}}$ according to the following distributions

$$f(m_{\text{cut off}}) \propto e^{-b_1 m_{\text{cut off}}} \quad \text{with} \quad m_0 < m_{\text{c.o.}} < \infty, \tag{14}$$

$$f(p^2_{\text{cut off}}) \propto e^{-b_2 p^2_{\text{cut off}}} \quad \text{with} \quad 0 \leqslant p_{\text{c.o.}} < \infty, \tag{15}$$

and get

$$E_{\text{cut off}} = \sqrt{p^2_{\text{cut off}} + m^2_{\text{cut off}}}\,. \tag{16}$$

The lower limit m_0 of the cut off mass is necessary to guarantee that the cut off energy is not lower than the mass of the hadron which can be emitted from the incoming quark jet. So we get

$$m_0 = \begin{cases} m_q \text{ for u or d quarks in the incoming jet,} \\ m_{K^*} \text{ for s quarks in the incoming jet.} \end{cases} \tag{17}$$

This method allows us to regulate the multiplicities of the final hadron states by varying the parameters b_1 and b_2 in the above distributions. With the values $b_1 = 8.0\,\text{GeV}^{-1}$ and $b_2 = 8.0\,\text{GeV}^{-2}$ we get a good agreement with experimental data.

3.2. Choice of the vertex

In this step we determine whether a meson or (anti) baryon should be emitted in the next step. The ratio between meson and baryon production is specified by weights α_B and α_M with $\alpha_B + \alpha_M = 1$, where α_B and α_M are the probabilities to choose a baryon or meson vertex. From comparison with data [8] we find for the ratio of these probabilities

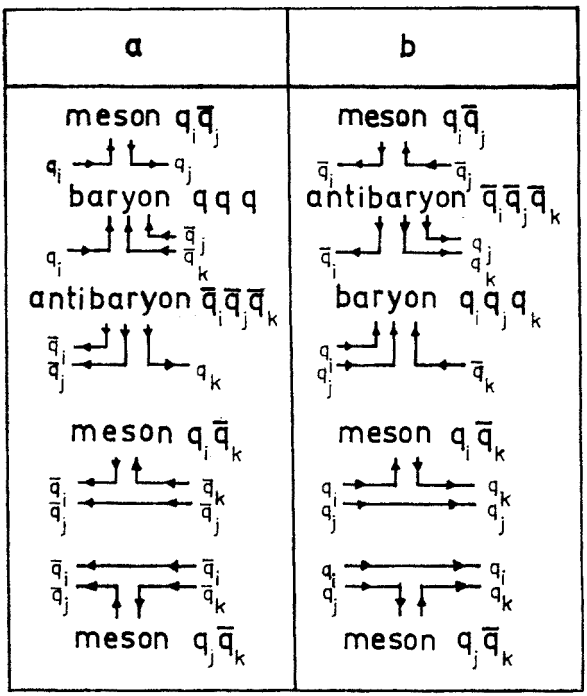

Fig. 6. All possible vertices for meson, baryon and antibaryon production in our chain decay model. a) in the jet of the primary quark q_0; b) in the jet of the primary antiquark $\bar{q}_0$. i, j, k are the flavour indices

$\alpha_B/\alpha_M \approx 0.05$. In figure 6 one can see all possible vertices in dependence on the original quark q or $\bar{q}$. When choosing the vertex we have to take into account that the chosen vertex must start with the secondary constituent of the previous vertex.

3.3. Choice of the quark flavour

We sample quark flavours in our model by introducing probabilities $P_{q\bar{q}}$ for the formation of different $q\bar{q}$ pairs. Depending on the chosen vertex we have to create one or two $q\bar{q}$ pairs. Field and Feynman [1] used the following probabilities $P_{q\bar{q}}: P_{u\bar{u}} = P_{d\bar{d}} = 0.4$ and $P_{s\bar{s}} = 0.2$. We calculate these probabilities $P_{q\bar{q}}$ according to the following mass dependent distribution:

$$P_{q\bar{q}} = \begin{cases} C \int_{m_q}^{E_R} 2E_\perp e^{-bE_\perp} dE_\perp & \text{for } E_R > m_q, \\ 0 & \text{for } E_R \leqslant m_q. \end{cases} \tag{18}$$

C is a normalization constant determined in accordance to the sum rule $\sum_q P_{q\bar{q}} = 1$ and E_R is the energy in the incoming (anti) quark jet or (anti) diquark jet. For constituent quark masses $m_u = m_d \approx 0.3$ GeV, $m_s \approx 0.5$ GeV and $m_c \approx 2.1$ GeV we get with $b = 6.0$ GeV^{-1} the following probabilities: $P_{u\bar{u}} = P_{d\bar{d}} = 0.41$, $P_{s\bar{s}} = 0.179$ and $P_c = 0.0001$.

3.4. Classification of the hadrons

Depending on the chosen vertex and quark flavours a meson $q_i\bar{q}_j$ or baryon $q_iq_jq_k$ or antibaryon $\bar{q}_i\bar{q}_j\bar{q}_k$ has been created. The following lowest meson and (anti)baryon multiplets of the symmetry group SU(3) are used for the hadron classification: (*i*) pseudoscalar meson nonet (PS), (*ii*) vector meson nonet (V), (*iii*) baryon and antibaryon octet (B8, A8), (*iv*) baryon and antibaryon decuplet (B10, A10). These multiplets obtain the most important stable and unstable hadrons of the symmetry group SU(3). The ratios between members of the same multiplet are given by the corresponding Clebsch-Gordan coefficients and the ratios between different multiplets are specified by weights α_{PS}, α_V with $\alpha_{PS} + \alpha_V = 1$ and α_{B8}, α_{A8}, α_{A10}, α_{B10} with $\alpha_{A8} = \alpha_{B8}$, $\alpha_{A10} = \alpha_{B10}$ and $\alpha_{B8} + \alpha_{B10} = 1$. SU(6) suggests ratios of different multiplets determined by the spin of its members $\alpha_{PS}/\alpha_V = 1/3$ and $\alpha_{B8}/\alpha_{B10} = \alpha_{A8}/\alpha_{A10} = 1/2$.

3.5. Choice of the energy

Field and Feynman [1] used the momentum sharing function

$$f(z') = 1 - a + 3a(1 - z')^2 \quad \text{with } a = 0.88. \tag{19}$$

Ilgenfritz, Kripfganz and Schiller [2] used

$$f(z') = (n+1)(1-z')^n \quad n \geqslant 1, \tag{20}$$

where n is the number of the elementary constituents in the residual jet. The scaling variable is defined as $z' = \dfrac{p_{\text{hadron}}}{p_{\text{quark jet}}}$. Instead of the momentum fraction z' we choose the energy fraction $z = \dfrac{E_{\text{hadron}}}{E_{\text{jet}}}$. Therefore we use the following energy sharing function.

$$f(z) = 1 - a + 3a(1-z)^b. \tag{21}$$

$b = 1$ is for a meson vertex and $b = 2$ for a baryon or antibaryon vertex. For the parameter a we use the value 0.88 [1].

3.6. Inclusion of the transverse momentum

We include the transverse momentum in our model by giving each emitted hadron h a transverse momentum according to the distribution

$$\frac{d\sigma}{dE_\perp} \propto 2E_\perp \cdot \exp(-E_\perp d) \quad \text{with} \quad E_\perp = \sqrt{\vec{p}_{\perp h}^2 + m_h^2} - m_h, \tag{22}$$

where m_h is the mass of the hadron. The transverse momentum conservation in each emission step demands

$$\vec{p}_{\perp i-1} = \vec{p}_{\perp hi} + \vec{p}_{\perp i}. \tag{23}$$

$\vec{p}_{\perp i-1}$ and $\vec{p}_{\perp i}$ are the transverse momenta of the incoming and outgoing constituents in the i-th emission step and $\vec{p}_{\perp hi}$ is the chosen transverse momentum of the emitted hadron. In case of a simple meson vertex we have

$$\vec{p}_{\perp hi} = \vec{p}_{\perp qi-1} + \vec{p}_{\perp \bar{q}i}, \tag{24}$$

and hence with equation (23)

$$\vec{p}_{\perp qi-1} = \vec{p}_{\perp qi-1} + \vec{p}_{\perp \bar{q}i} + \vec{p}_{\perp qi}. \tag{25}$$

That means the conservation of the transverse momentum of each newly created $q\bar{q}$ pair

$$\vec{p}_{\perp qi} + \vec{p}_{\perp \bar{q}i} = 0. \tag{26}$$

For the parameter d in the distribution (22) we use the value $d = 6.0\ \text{GeV}^{-1}$ and get average hadron transverse momenta which depend on the masses. For pions we obtain $\langle p_\perp \rangle = 0.3$ to $0.4\ \text{GeV}/c$.

3.7. Combination of the two hadron jets

When the chain decay of the two separate quark jets with the original quark q and antiquark $\bar{q}$ are terminated we compose all already emitted hadrons and the two residual jets of these quark jets into a two-jet which conserves energy momentum and quantum numbers exactly. The energy and momentum of the two combined residual jets is determined by the energy-momentum conservation for the jet

$$\sum_i E_{hi} + E_{\text{residual jet}} = \sqrt{s}, \tag{27}$$

$$\sum_i \vec{p}_{hi} + \vec{p}_{\text{residual jet}} = 0. \tag{28}$$

The sum goes over all hadrons emitted so far. The residual jet may contain one or two last particles depending on its quark constituents. These last one or two hadrons carry well defined masses by their classification. On the other hand their energy and momentum is exactly determined by the energy-momentum conservation for the whole jet. Hence we get a contradiction if the residual jet contains only one particle since its mass is then double defined. In such cases we include one of the already emitted hadrons in the last kinematical calculations. Thus we are able to conserve exactly energy and momentum for the whole jet. Due to the virtual quark masses which we never need to specify in our calcu-

lations we are not able to exclude events in which the invariant mass of the residual jets is less than the sum of the masses of the one or two last hadrons inside of this residual system. It may even happen that the energy of the residual system is less than its momentum. We reject such events.

3.8. Decay of hadron resonances

We are interested in hadron final states which contain only stable hadrons. For the simulation of the decay of the emitted resonances into stable final hadrons we use a computer program [9]. In this program each resonance might have several decay channels. The ratios between these decay channels are taken from the particle data group tables [10] and only decay channels are used with branching ratios bigger than 1%.

4. Discussion of the Monte Carlo results and comparison with experimental data

In this chapter we discuss the comparison of the Monte Carlo chain decay calculations with experimental data from SLAC and DESY [8], [11–24]. Since charmed hadrons and hadronic decays of heavy leptons are not yet included we do not expect complete agreement with data above $\sqrt{s} = 4.0$ GeV.

4.1. Multiplicity distributions

We expect a logarithmic increase of the average secondary hadron multiplicity as function of the center of mass energy. Figure 7 shows the average multiplicities of all hadrons and only charged hadrons versus the center of mass energy compared with data

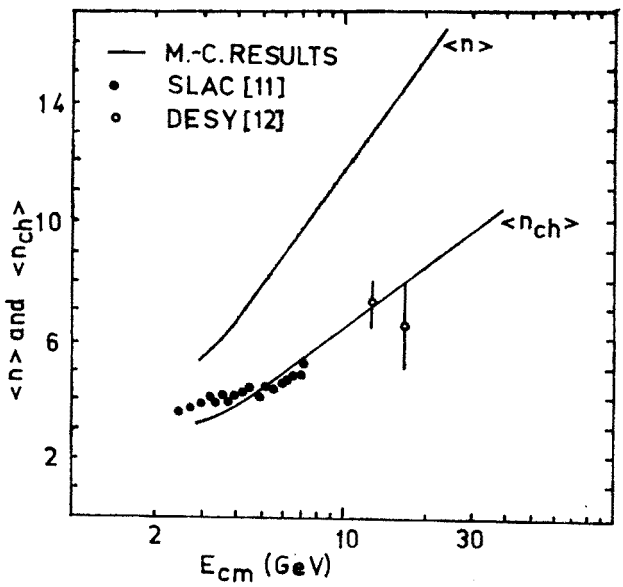

Fig. 7. Average multiplicities of all hadrons and charged hadrons versus E_{cm}. The Monte Carlo results are compared with data from SLAC [11] and DESY [12]

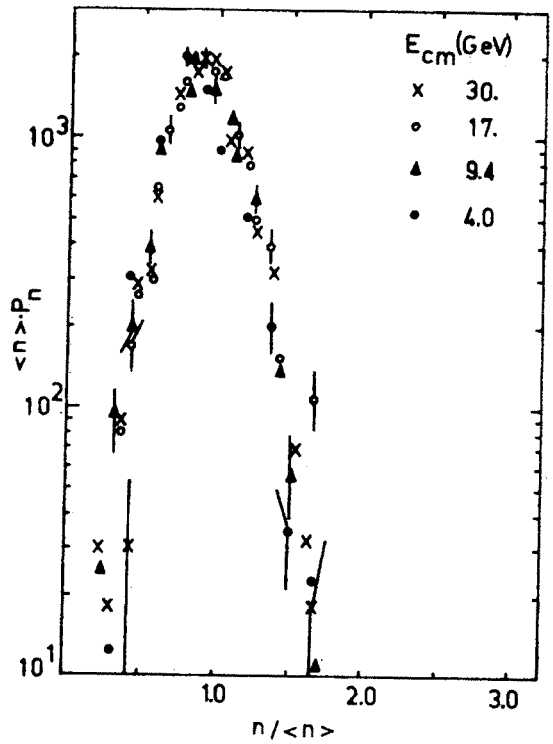

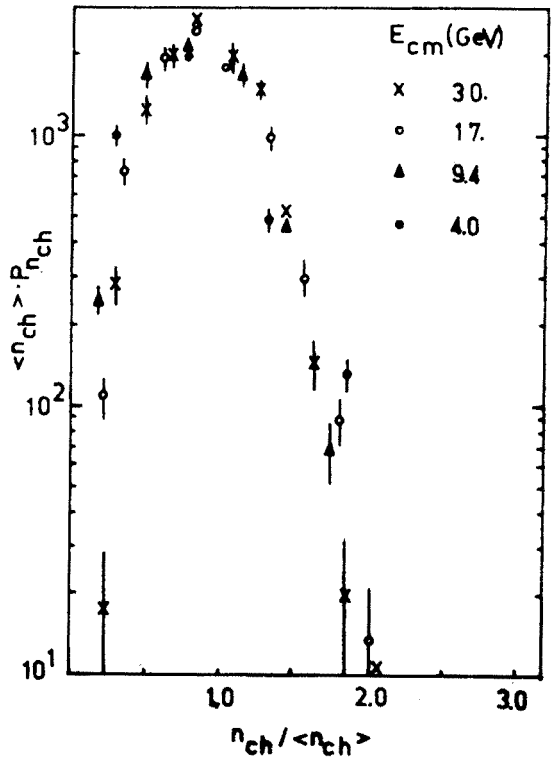

Fig. 8a) Multiplicity distributions of all hadrons for several center of mass energies. P_n is the relative number of events with multiplicity n; $\langle n \rangle$ is the average multiplicity. b) Multiplicity distributions of all charged hadrons for several center of mass energies. $P_{n_{ch}}$ is the relative number of events with charged particle multiplicity n_{ch}. $\langle n_{ch} \rangle$ is the average charged particle multiplicity. The distributions show approximate KNO scaling [27]

from SLAC [11] and DESY [12]. The two free parameters for the cut-off energy distribution (equations (14)–(16)) have been chosen as $b_1 = b_2 = 8.0\ \mathrm{GeV}^{-1}$.

Above 5.0 GeV the Monte Carlo data seem to be somewhat higher than the experimental data. The inclusion of charm and heavy leptons should provide a better agreement above 4 or 5 GeV since the decays of heavy leptons and charmed hadrons provide final states with lower multiplicities.

In figures 8a and 8b we plot the multiplicity distributions of all particles and only charged particles, respectively, and find approximate KNO-scaling in the energy range $\sqrt{s} = 4$ to 30 GeV.

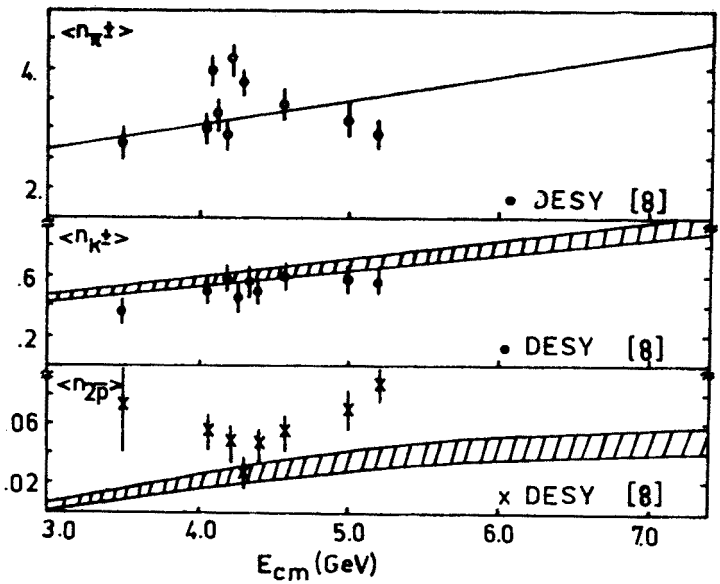

Fig. 9. Average multiplicities for charged pions, kaons and twice of the antiprotons as function of the center of mass energy compared with data from DESY [8]. In case of kaons and antiprotons we have plotted a hatched region which represents the statistical error of the Monte Carlo calculations

In figure 9 we show the average multiplicities for charged pions, kaons and antiprotons compared with data from DESY [8]. We are not able to provide complete agreement with the data, however, the multiplicity ratios between pions, kaons and antiprotons agree reasonably well with the data.

4.2. Energy and momentum distributions

Next we discuss average energies and momenta as function of the center of mass energy as well as energy and momentum distributions.

In figure 10 we plot the average energy carried by all charged particles devided by the total jet energy versus the center of mass energy. Experimental data [11] decrease approximately from 0.6 to 0.5 in the energy range $\sqrt{s} = 2.6$ GeV to $\sqrt{s} = 8.0$ GeV. Our model provides a ratio which decreases less rapidly.

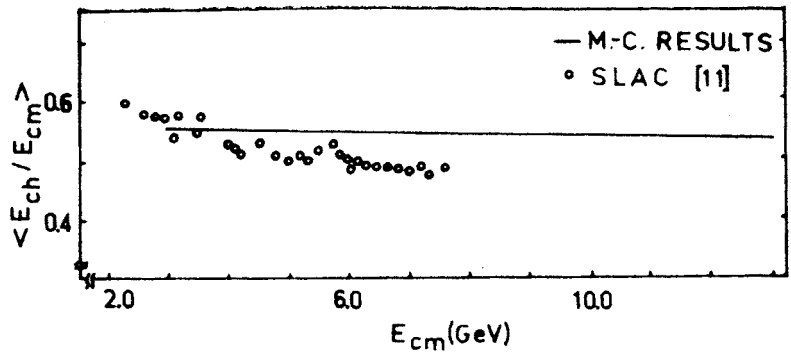

Fig. 10. Average energy of all charged hadrons divided by the total jet energy in dependence of the center of mass energy compared with data from SLAC [11]

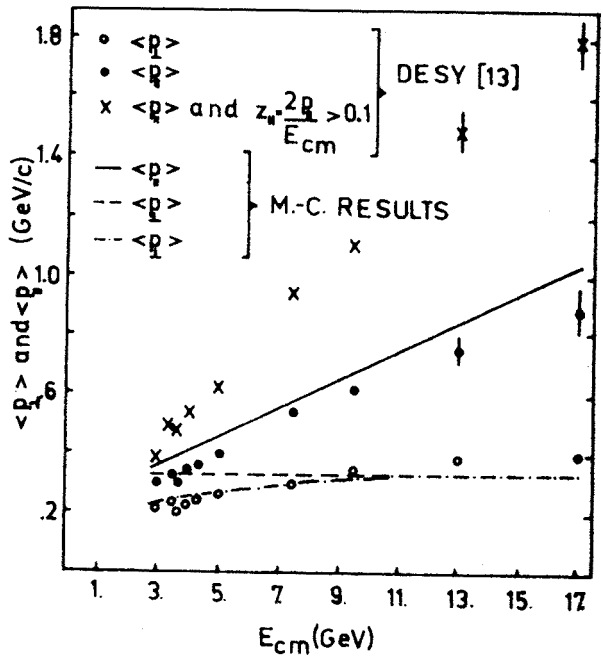

Fig. 11. Average transverse (dash-dot line) and longitudinal (continuous line) momenta relative to the jet axis versus E_{cm} compared with data from DESY [13]. In our Monte Carlo calculations we identify the jet axis with the thrust axis. Additionally we show the average transverse momenta (hatched line) relative to the direction of the primary $q\bar{q}$ pair

This may be due to the fact that all final charged particles are considered as pions in the experiment. Since we know the exact number of charged pions, kaons, protons and antiprotons in the final hadronic state in our calculations we get no energy loss by incorrect particle identification. On the other hand the flavour and energy choice for the emitted hadrons is independent of the total jet energy in our model and all effects which

cause a decrease of the above ratio should only be effected by the resonance decay mechanism. In figure 11 we compare the average transverse and longitudinal momenta relative to the jet axis with data from DESY [13]. We identify the jet axis with the thrust axis in our calculations, which is found for each event by an iterative method.

For the free parameter of the transverse energy distribution (equation (22)) we use the value $d = 5.8\ \mathrm{GeV}^{-1}$. In general there is a good agreement with data. The average transverse momenta provided by the model might be somewhat too low and the longitudinal momenta somewhat too high compared with the data. This could be corrected by the choice of a lower value for the free parameter d, however, if we later include charm and heavy lepton production in the model we get more particles with higher transverse momenta

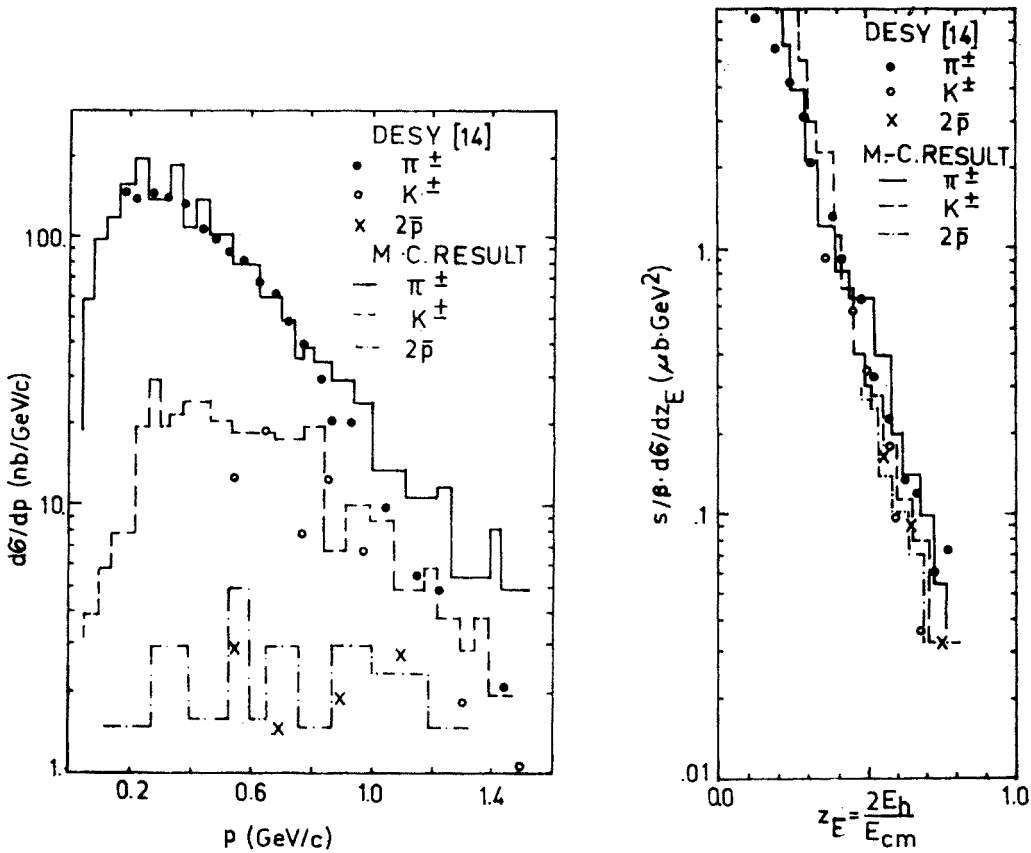

Fig. 12a) $\frac{d\sigma}{dp}$ versus p for $\pi^{\pm}$, $K^{\pm}$ and $2\bar{p}$ at $E_{cm} = 4.0$ GeV compared with data from DESY [14] at $3.98 < E_{cm} < 4.10$ GeV. For comparison with data we have normalized the calculated distributions using the experimental hadronic cross section [14]; b) $\frac{s}{\beta}\frac{d\sigma}{dz_E}$ versus $z_E = \frac{2E}{\sqrt{s}}$ for $\pi^{\pm}$, $K^{\pm}$ and $2\bar{p}$ at $E_{cm} = 4.0$ GeV compared with data from DESY [14] at $3.98 < \sqrt{s} < 4.10$ GeV. For comparison with data we have normalized the calculated distributions using the experimental hadronic cross section [14]

and lower longitudinal momenta, respectively, since we use a mass dependent transverse energy distribution (equation (22)). In figure 11 we also show the average transverse momenta relative to the direction of the primary quark antiquark pair which we know of course in our calculations in contrast to the experiment.

If we compare the average transverse momenta relative to the thrust axis and relative to the direction of the primary $q\bar{q}$ pair we get a good agreement for energies above $\sqrt{s} = 9.0$ GeV. For lower center of mass energies the average transverse momenta relative to the thrust axis decrease and the ones relative to the primary $q\bar{q}$ direction are independent of the center of mass energy. This is what we expect since the jet axis and the axis of the primary $q\bar{q}$ pair agree better and better with increasing center of mass energies.

Figures 12a and 12b show distributions for charged pions, kaons and antiprotons versus their momenta p and their energy fraction $z_E = \frac{2E}{\sqrt{s}}$, respectively for $\sqrt{s} = 4.0$ GeV

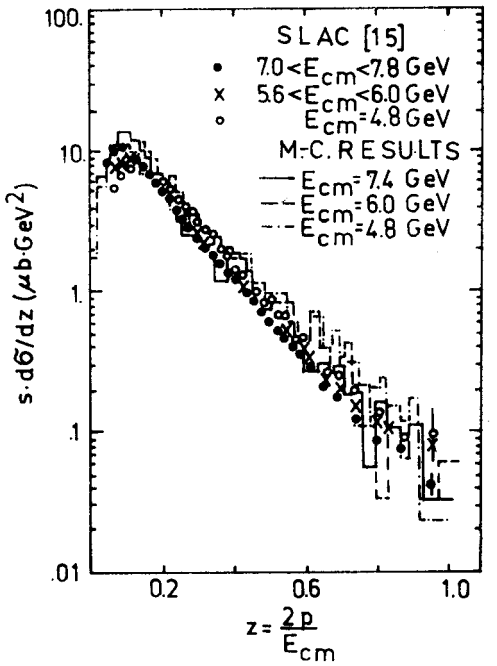

Fig. 13

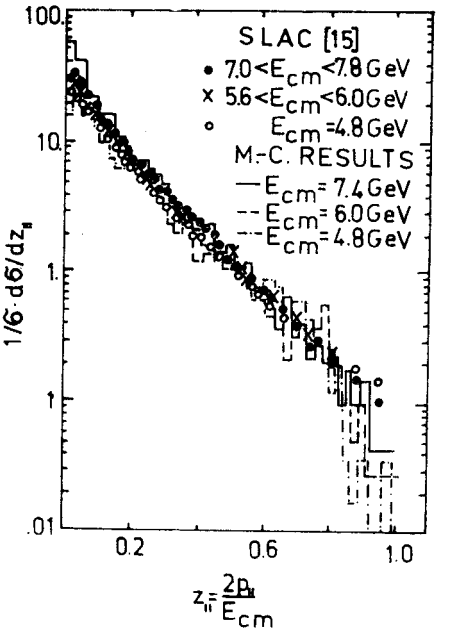

Fig. 14

Fig. 13. Momentum fraction distributions $\frac{1}{\sigma}\frac{d\sigma}{dz}$ versus $z = \frac{2p}{\sqrt{s}}$ for charged hadrons at several center of mass energies compared with data from SLAC [15]. The Monte Carlo distributions are normalized according to the data using the experimental hadronic cross section [14]

Fig. 14. Momentum fraction distributions $\frac{1}{\sigma}\frac{d\sigma}{dz_\parallel}$ versus $z_\parallel = \frac{2p}{\sqrt{s}}$ for charged hadrons at several center of mass energies compared with data from SLAC [15]. The Monte Carlo distributions are normalized according to the data

compared with data from DESY [14] at 3.98 GeV $< \sqrt{s} <$ 4.10 GeV. In order to compare the Monte Carlo distributions with experimental data of the form $\frac{d\sigma}{dp}$ and $\frac{s}{\beta}\frac{d\sigma}{dz_E}$ we normalize the Monte Carlo data using the experimental hadronic cross-section [14]. The agreement with data is good.

In figures 13 and 14 we get a similar good agreement with data from SLAC [15] for the distributions $s\frac{d\sigma}{dz}$ versus $z = \frac{2p}{\sqrt{s}}$ and $\frac{1}{\sigma}\frac{d\sigma}{dz_\parallel}$ versus $z_\parallel = \frac{2p_\parallel}{\sqrt{s}}$ at several centers of mass energies. Due to the fact that we neglect heavy lepton and charm production we cannot expect complete agreement with data.

In figure 15 we plot the quark fragmentation functions for u-quarks into π^+ and π^-. The results of the model are compared with data from νp, $\bar{\nu}$p [16] and ep [17] lepton-

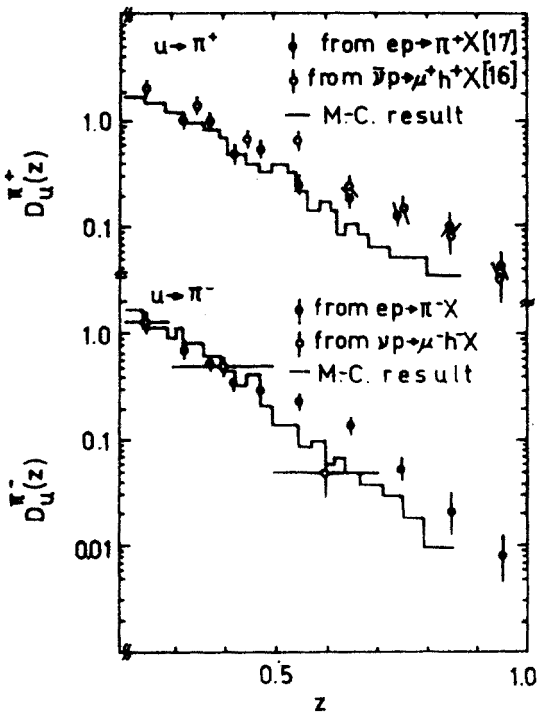

Fig. 15. Fragmentation functions of u quarks into π^+ and π^-. The caulculated fragmentation functions are compared with data from νp and $\bar{\nu}$p experiments [16] and ep experiments [17] in the kinematic region $12 < W^2 < 16\,\text{GeV}^2$, $2 < Q^2 < 6\,\text{GeV}^2$, $0.1 < x < 0.45$ and $0.2 \leqslant z \leqslant 0.9$

nucleon scattering events in the kinematic region $2 < Q^2 < 6\,\text{GeV}^2$, $0.1 < x < 0.45$, $12 < W^2 < 16\,\text{GeV}^2$ and $0.2 \leqslant z \leqslant 0.9$. W is the invariant mass of the final state hadrons, $-Q^2$ and ν are the invariant mass squared and laboratory energy of the virtual photon and $x = \frac{Q^2}{2M\nu}$. Since our model shows a relatively good scaling behaviour for center

of mass energies above 4.0 GeV (figures 13 and 14) we are able to compare our calculated fragmentation functions with data from lepton–nucleon scattering events for z values above 0.2. In the $\bar{\nu}$p-scattering experiment [16] $D_u^{h^+}(z)$ is measured. In our model we determine $D_a^{\pi^+}(z)$. Therefore our calculated fragmentation functions might be somewhat lower than the data from $\bar{\nu}$p-scattering events.

4.3. Thrust and sphericity distributions

For the analysis of the jet character of the hadronic final states in e^+e^--annihilation we use the well known thrust variable, which is defined as [18, 19]:

$$T = \max \{\sum_i |\vec{p}_{\parallel i}| / \sum_i |\vec{p}_i|\} \quad \text{with} \quad \tfrac{1}{3} \leqslant T \leqslant 1. \tag{29}$$

The sum goes over all final particles and the longitudinal momenta $\vec{p}_{\parallel i}$ are defined relative to the jet axis $\vec{e}$ by $\vec{p}_{\parallel i} = \vec{p}_i \cdot \vec{e}$. $T = 1$ belongs to an ideal two jet event and $T = \frac{1}{3}$ belongs to an isotropic event. Furthermore, we consider the sphericity [20]:

$$\hat{S} = \tfrac{3}{2} \min \{\sum_i \vec{p}_{\perp i}^2 / \sum_i \vec{p}_i^2\} \quad \text{with} \quad 0 \leqslant \hat{S} \leqslant 1. \tag{30}$$

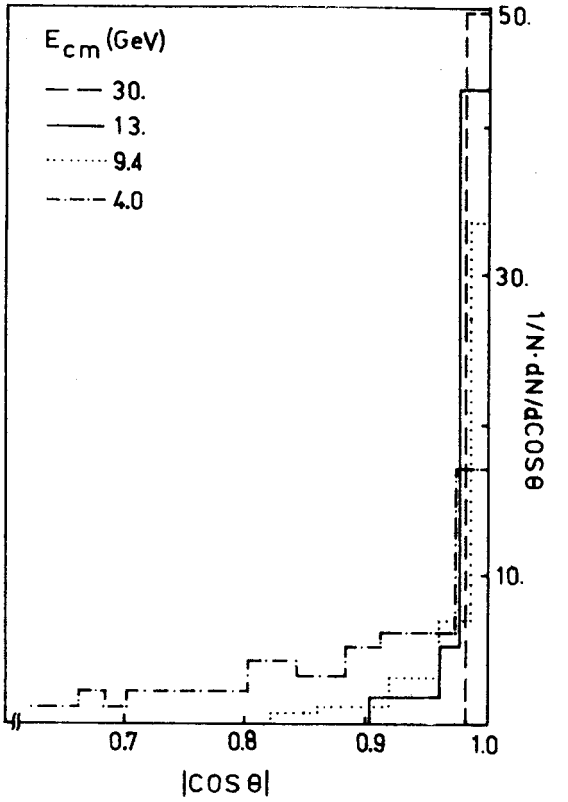

Fig. 16. Calculated angular distributions $\frac{1}{N} \frac{dN}{d\cos\theta}$ versus $|\cos\theta|$ for several center of mass energies. θ is the angle between the thrust axis and the direction of the primary $q\bar{q}$ pair. The distributions are normalized to the number of events N at each energy

$\hat{S} = 0$ belongs to an ideal two jet event and $\hat{S} = 1$ belongs to an isotropic event. Sphericity distributions have been studied in detail experimentally [22, 23]. We determine the thrust values by an iterative method. At high enough center of mass energies the jet axis agrees approximately with the direction of the primary quark antiquark pair. Starting with this direction we need only a small correction in order to find the thrust axis. An iterative method to calculate this correction works very well.

In figure 16 we present the angular distribution of the thrust axis in the center of mass system $\frac{1}{N}\frac{dN}{d\cos\theta}$ versus $|\cos\theta|$ for several center of mass energies. θ is the angle between the thrust axis and the primary $q\bar{q}$ pair direction. The agreement between these two directions is indeed a good one for high enough center of mass energies. Since we use only two jet events and neglect contributions from three and more jet events and neglect also contributions from charmed meson and heavy lepton decays we cannot expect complete agreement with data.

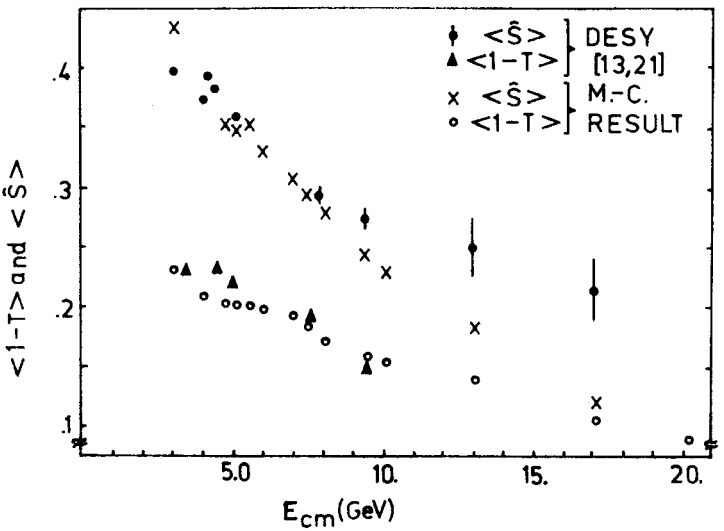

Fig. 17. Average sphericity $\langle\hat{S}\rangle$ and thrust $\langle 1-T\rangle$ versus the center of mass energy compared with data from DESY [13, 21]

In figure 17 we have plotted the average sphericity $\langle\hat{S}\rangle$ and the average thrust $\langle 1-T\rangle$ versus the center of mass energy. For the energy range between 2 GeV and 8 GeV we have a good agreement with data from DESY [13, 21].

In figures 18a, b and c we compare the sphericity distributions $\frac{1}{N}\frac{dN}{d\hat{S}}$ for the center of mass energies $E_{cm} = 9.4$ GeV, 13.0 GeV and 17.0 GeV with data from the PLUTO Collaboration [22] and the TASSO Collaboration [23]. At $E_{cm} = 17.0$ GeV we observe a disagreement between our distribution and the data at large $\hat{S}$ values (Fig. 18c). Such a disagreement was interpreted recently as evidence for bottom decays [24].

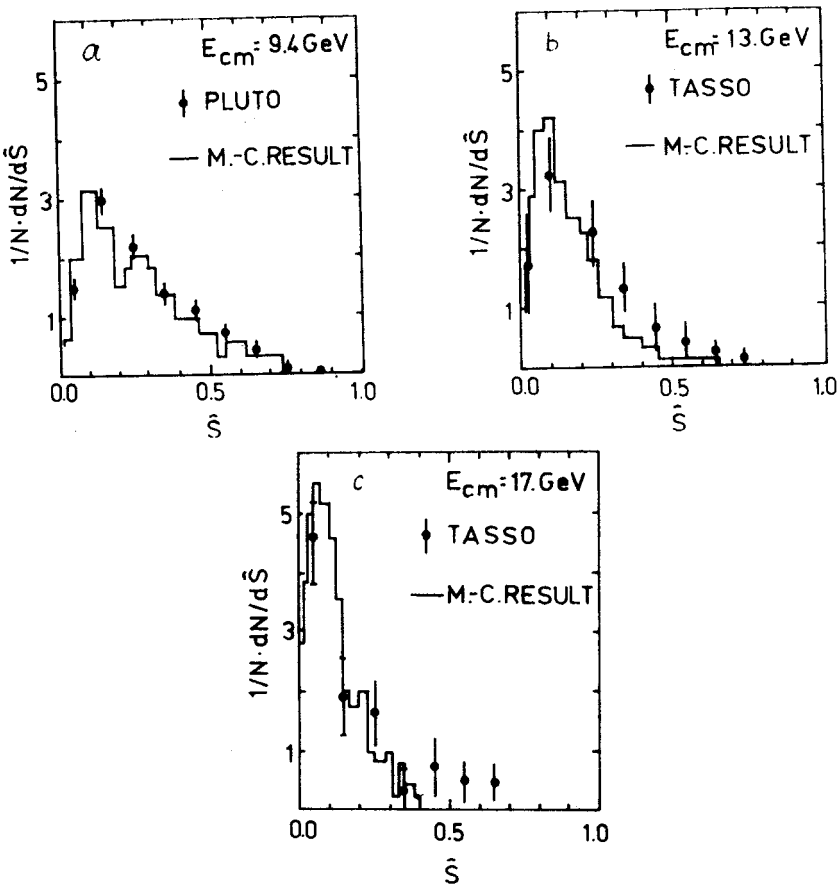

Fig. 18a) Sphericity distributions $\frac{1}{N}\frac{dN}{d\hat{S}}$ versus $\hat{S}$ for $E_{cm} = 9.4$ GeV compared with data from DESY [22, 23]. The distributions are normalized to the number of events N at the considered center of mass energy; b) The same like in figure 18a but for $E_{cm} = 13.0$ GeV; c) The same like in figure 18a but for $E_{cm} = 17.0$ GeV

In figure 19 we plot the calculated thrust distributions $\frac{1}{N}\frac{dN}{dT}$ versus T for several center of mass energies. With increasing center of mass energy the maximum of the distributions goes to $T = 1$ and the curves become more narrow. A possible analytical parametrization of the tail of these thrust distributions is [25]

$$\frac{dN}{dT} \sim \frac{1-T}{\Delta T^2} \exp\left(-\frac{1-T}{\Delta T}\right), \tag{31}$$

with $\Delta T = \frac{c \cdot \ln W}{W}$ [26] where W is the total hadronic energy of the event. We found a reasonable good fit for $c = 0.2293$.

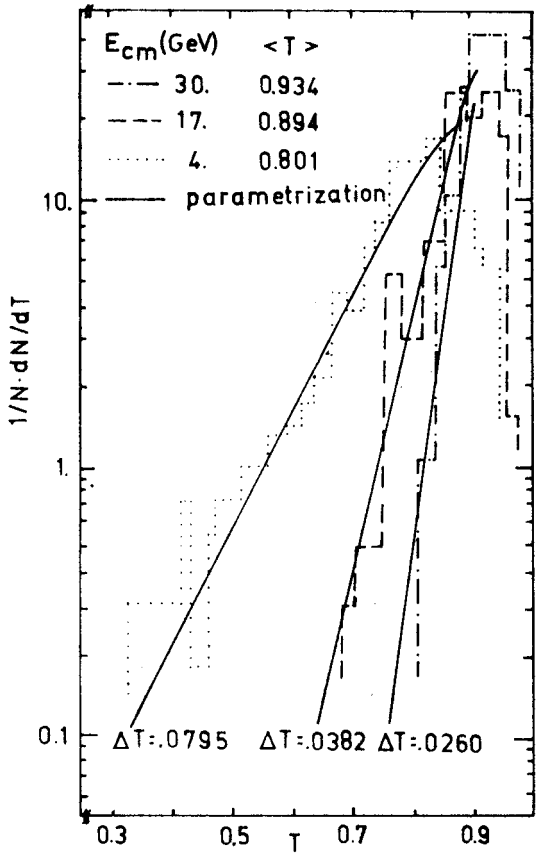

Fig. 19. Calculated thrust distributions $\frac{1}{N}\frac{dN}{dT}$ versus T for several center of mass energies. The distributions are normalized to the number of events N at each energy. We also compare these distributions with an analytical parametrization of the form $\frac{dN}{NT} \sim \frac{(1-T)}{\Delta T^2} \exp\left(-\frac{(1-T)}{\Delta T}\right)$ [25] with $\Delta T = 0.2293\,(\ln W)/W$. W is the total hadronic energy

5. *Summary*

In the present paper we have described a quark jet fragmentation model with the following features: (*i*) Inclusion of baryon and antibaryon production beside meson production, (*ii*) Conservation of energy and momentum of $q\bar{q}$ fragmentation events, (*iii*) Conservation of quantum numbers like Q, I_3, S and B, (*iv*) Inclusion of transverse momenta, (*v*) Fragmentation via meson and baryon resonances of the lowest SU(3) multiplets. We do not consider charmed hadrons and heavy leptons at this stage. In general the agreement with experimental data is good.

REFERENCES

[1] R. D. Field, R. P. Feynman, *Nucl. Phys.* **B136**, 1 (1978).
[2] E. M. Ilgenfritz, J. Kripfganz, A. Schiller, *Acta Phys. Pol.* **B9**, 881 (1978).
[3] F. Niedermayer, *Nucl. Phys.* **B79**, 355 (1974).
[4] J. Finkelstein, R. D. Peccei, *Phys. Rev.* **D6**, 2606 (1972).
[5] A. Krzywicki, B. Peterson, *Phys. Rev.* **D6**, 2606 (1972).
[6] U. P. Sukhatme, Orsay preprint LPTPE 77/38 (1977).
[7] U. P. Sukhatme, Cambridge preprint DAMTP 77/25 (1977).
[8] R. Brandelik et al., DASP Collaboration, DESY preprint DESY 78/50 (1978).
[9] K. Hänßgen, R. Kirschner, J. Ranft, S. Ritter, H. Wetzig, Leipzig preprint KMU (in preparation).
[10] C. Brinceman et al., *Particle Data Group, Review of Particle Properties, Phys. Lett.* **75B** (1978).
[11] R. Schwitters, Stanford Conference 1975, p. 5.
[12] Ch. Berger et al., PLUTO Collaboration, DESY preprint DESY 79/06 (1979).
[13] A. Klovning et al., PLUTO Collaboration, DESY preprint DESY 79/11 (1979).
[14] B. H. Wiik, G. Wolf, DESY preprint DESY 78/23 (1978).
[15] G. G. Hanson, SLAC preprint SLAC-PUB-2118 (1979).
[16] M. Derrick et al., preprint ANL-HEP-PR-77-39 (1977); J. C. Vander Velde, Proceedings of the Flaine Conference 1977, p. 365.
[17] G. Drews et al., DESY preprint DESY 78/34 (1978).
[18] E. Fahri, *Phys. Rev. Lett.* **39**, 1587 (1977).
[19] A. De Rujula et al., *Nucl. Phys.* **B138**, 387 (1978).
[20] G. Hanson, *Phys. Rev. Lett.* **39**, 1237 (1977).
[21] Ch. Berger et al., PLUTO Collaboration, DESY preprint 78/39 (1978).
[22] Ch. Berger et al., PLUTO Collaboration, DESY preprint DESY 78/71 (1978).
[23] R. Brandelik et al., TASSO Collaboration, DESY preprint DESY 79/14 (1979).
[24] A. Ali, J. G. Körner, G. Kramer, DESY preprint DESY 79/16 (1979).
[25] J. Ranft, G. Ranft, Leipzig preprint KMU-HEP-78-15 (1978), to be published in *Phys. Lett.* B.
[26] A. De Rujula, J. Ellis, E. G. Floratos, M. K. Gaillard, CERN preprint CERN-TH-2455 (1978).
[27] Z. Koba, H. B. Nielsen, P. Olesen, *Nucl. Phys.* **B40**, 317 (1972).